

Supplementary Materials

Text S1. Electrosorption isotherm

The electrosorption isotherm of the cell AC/MC-2 in different initial NaCl concentrations is investigated by the Langmuir and Freundlich isotherms models, and the used equations are as follows:

$$q_e = \frac{q_m K_L C_e}{1 + K_L C_e} \quad (S1)$$

$$q_e = K_F C_e^{1/n} \quad (S2)$$

where q_e and q_m (mg g^{-1}) are the equilibrium and maximum electro-sorptive capacity of NaCl. C_e (mg L^{-1}) is the equilibrium adsorption concentration. K_L (min^{-1}) is a Langmuir constant. K_F ($\text{mol}^{1-n} \cdot \text{L}^n \cdot \text{g}^{-1}$) and n (1) are the Freundlich constants.

Text S2. The electrosorption kinetics model

The electrosorption kinetics models are employed to analyze the electrosorption rates of the four cells in the CDI process. Here, the experimental data is fitted by the pseudo-first-order and pseudo-second-order models. The used kinetic models are expressed as below:

$$q_t = q_e (1 - e^{-k_1 t}) \quad (S3)$$

$$q_t = \frac{k_2 q_e^2 t}{1 + k_2 q_e t} \quad (S4)$$

where q_e (mg g^{-1}) and q_t (mg g^{-1}) refer to the electrosorption capacity of NaCl at equilibrium state and time t (min), respectively. K_1 (min^{-1}) and K_2 ($\text{g mg}^{-1} \text{min}^{-1}$) are the pseudo-first-order and pseudo-second-order rate constants, respectively.

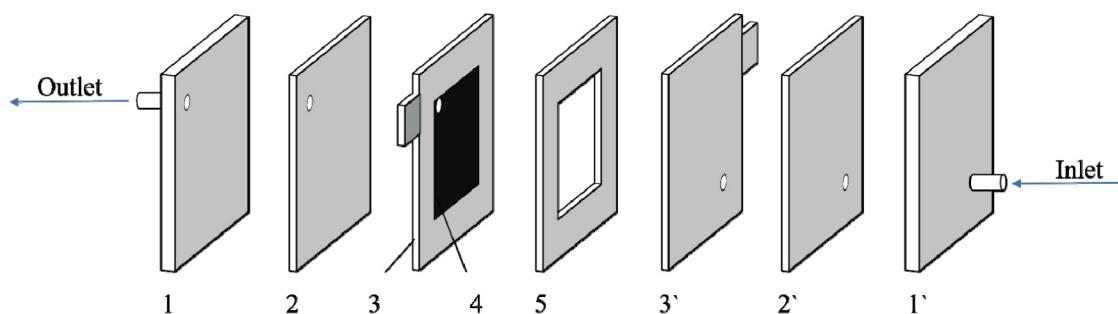


Fig. S1. Electro-sorption cell in this work. 1,1`-Support plate(organic glass). 2,2`-Silicon rubber gasket. 3,3`-Aluminium plate. 4.-Active material. 5.-Silicon rubber spacer.

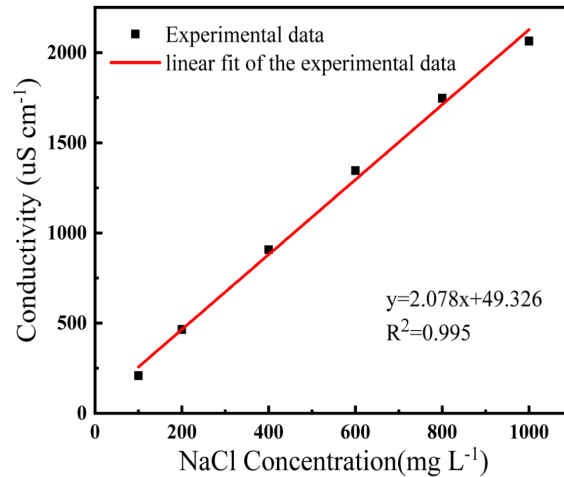


Fig. S2. The relationship between the concentration and conductivity of NaCl solution.

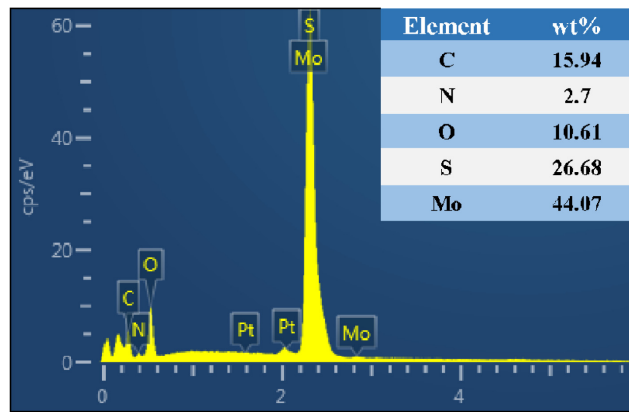


Fig. S3. EDS analysis of MC-2 material.

Table S1. Parameters and correlation coefficients of Langmuir and Freundlich isotherm models for AC//MC-2 cell.

q_{\max} (mg/g)	Langmuir			Freundlich		
	K_L (min^{-1})	R^2	n	K_F ($\text{mol}^{1-n} \cdot \text{L}^n/\text{g}$)	R^2	
58.73	0.0017	0.9818	1.3	0.4258	0.9870	

Table S2. The kinetics parameters of pseudo-first-order and pseudo-second-order models for the four cells.

Sample	q_{exp} (mg/g)	pseudo-first-order model			pseudo-second-order model		
		q_e (mg/g)	k_1 (1/min)	R^2	q_e (mg/g)	k_2 (g/(mg·min))	R^2
AC//MoS ₂	23.69	23.40	0.1186	0.9945	28.00	0.0051	0.9868
AC//MC-1	17.27	17.16	0.0946	0.9809	21.76	0.0048	0.9630
AC//MC-2	29.14	28.80	0.1395	0.9859	33.53	0.0053	0.9663
AC//MC-3	21.76	21.52	0.0898	0.9931	26.52	0.0036	0.9859

Table S3. Desalination performance comparison of MoS₂/CP and other reported materials.

Materials	Initial concentration (mg L ⁻¹)	Applied voltage (V)	SAC (mg g ⁻¹)	SAR (mg g ⁻¹ min ⁻¹)	Refs
Ce-MoS ₂	23400	1.2	8.81	0.22	[1]
T-MoS ₂	100	0.8	24.6	0.31	[2]
MoS ₂ /CNT	29200	0.8	25	0.42	[3]
MoS ₂ @CNT-CS	500	1.2	25.35	3.9	[4]
MoS ₂ /NOMC	250	1.6	28.82	0.72	[5]
MoS ₂ /g-C ₃ N ₄	250	1.6	24.16	0.81	[6]
3D flower-like MoS ₂ /rGO	200	1	16.82	0.56	[7]
MoS ₂ /rGO	300	1.4	34.2	3.05	[8]
MoS ₂ /PDA	200	1.2	16.94	1.69	[9]
MoS ₂ /CP	500	1.2	29.14	2.9	This work

References

1. Xing F, Li T, Li J, Zhu H, Wang N, Cao X. Chemically exfoliated MoS₂ for capacitive deionization of saline water. *Nano Energy* 2017;31:590-595. <https://doi.org/10.1016/j.nanoen.2016.12.012>.
2. Jia F, Sun K, Yang B, Zhang X, Wang Q, Song S. Defect-rich molybdenum disulfide as electrode for enhanced capacitive deionization from water. *Desalination* 2018;446:21-30. <https://doi.org/10.1016/j.desal.2018.08.024>.
3. Srimuk P, Lee J, Fleischmann S, Choudhury S, Jäckel N, Zeiger M, Kim C, Aslan M, Presser V. Faradaic deionization of brackish and sea water via pseudocapacitive cation and anion intercalation into few-layered molybdenum disulfide. *J. Mater. Chem. A* 2017;5:15640-15649. <https://doi.org/10.1039/C7TA03120C>.
4. Cai Y, Zhang W, Fang R, Zhao D, Wang Y, Wang J. Well-dispersed few-layered MoS₂ connected with robust 3D conductive architecture for rapid capacitive deionization process and its specific ion selectivity. *Desalination* 2021;520. <https://doi.org/10.1016/j.desal.2021.115325>.
5. Tian S, Zhang X, Zhang Z. Novel MoS₂/NOMC electrodes with enhanced capacitive deionization performances. *Chem. Eng. J.* 2021;409. <https://doi.org/10.1016/j.cej.2020.128200>.
6. Tian S, Zhang X, Zhang Z. Capacitive deionization with MoS₂/g-C₃N₄ electrodes. *Desalination* 2020;479:114348. <https://doi.org/10.1016/j.desal.2020.114348>.
7. Peng W, Wang W, Han G, Huang Y, Zhang Y. Fabrication of 3D flower-like MoS₂/graphene composite as high-performance electrode for capacitive deionization. *Desalination* 2020;473:114191. <https://doi.org/10.1016/j.desal.2019.114191>.
8. Gao L, Dong Q, Bai S, Liang S, Hu C, Qiu J. Graphene Oxide-Tuned MoS₂ with an Expanded Interlayer for Efficient Hybrid Capacitive Deionization. *Acs Sustainable Chem. Eng.* 2020;8:9690-9697. <https://dx.doi.org/10.1021/acssuschemeng.0c01453>.
9. Wang Q, Jia F, Song S, Li Y. Hydrophilic MoS₂/polydopamine (PDA) nanocomposites as the electrode for enhanced capacitive deionization. *Sep. Purif. Technol.* 2020;236. <https://doi.org/10.1016/j.seppur.2019.116298>.